Direct Measurement of the Polarized Optical Absorption Cross Section of Single-Wall Carbon Nanotubes

M. F. Islam, D. E. Milkie, C. L. Kane, A. G. Yodh, and J. M. Kikkawa

Department of Physics and Astronomy, University of Pennsylvania,
209 S. 33rd Street, Philadelphia, Pennsylvania 19104-6396, USA
(Received 12 December 2003; published 16 July 2004)

We determine optical absorption cross sections of single-wall carbon nanotubes for visible light copolarized and cross polarized with respect to the nanotube axis. The need for perfectly aligned ensembles in absorbance measurements is eliminated by using Raman scattering to measure the nematic order parameter in magnetically aligned nanotube suspensions. The absorbance data allow the first quantitative, spectral comparisons with theories of local field depolarization, and provide benchmark spectra for simple, rapid, and quantitative measurements of alignment within nanotube dispersions.

Single-wall carbon nanotubes (SWNTs) are unusual macromolecules that have thus far exhibited large electrical [1] and thermal [2] conductivities, extraordinary mechanical strength [3], and rich optical spectra [4–7]. Their substantial length-to-diameter aspect ratio presents a fundamental structural anisotropy that influences all these properties, in some cases depending strongly on the detailed arrangement of carbon atoms as indexed by the wrapping vector of the underlying graphene sheet [8]. Despite its fundamental interest, the polarized absorbance cross sections of carbon nanotubes have not been previously obtained. Prior absorbance measurements have revealed differences for light polarized parallel and perpendicular to an axis of alignment [6], but were difficult to relate to bare nanotube properties because, for example, the nanotube alignment was not well characterized. Our experiments demonstrate that perfectly aligned ensembles of nanotubes are *not necessary* to obtain absolute polarized absorbance cross sections. Instead, a combination of Raman scattering and linear optical absorbance can be used to extract the anisotropic optical absorbance spectra, even from samples that are weakly ordered. To our knowledge, this Letter presents the first measurements of absolute linear absorption cross sections for incident light polarized parallel and perpendicular to the nanotube axis.

These data enable us to rigorously test theories for absorptive processes [9,10], and provide the first direct confirmation that subband features are absent from the cross-polarized channel, as theoretically predicted. Moreover, these anisotropic spectra can be used as a benchmark for simple, rapid, and quantitative measurements of nanotube orientations, even when anisotropic reabsorption complicates Raman-based approaches. Since many potential applications of SWNTs [11] aim to utilize their individual anisotropic responses within bulk systems such as composites, broadly accessible methods for determining ensemble anisotropies are of great interest.

In this work, we weakly align SWNT suspensions in a magnetic field and subsequently lock them in place by suspension gelation. Polarized Raman scattering uniquely identifies a nematic order parameter (i.e., degree of nanotube alignment) for each sample, which combines with the absorbance data to recover the polarized absorbance spectra for a perfectly aligned ensemble of nanotubes. The resulting spectra are independent of nanotube concentration and degree of alignment and exhibit a contrast ratio of ~5 for light polarized parallel and perpendicular to the SWNT axis.

We prepare samples by purifying laser-oven nanotubes [12] in raw form according to a procedure largely described in Ref. [13]. X-ray and thermogravimetric analysis show the purified nanotubes contain >90 wt % SWNTs, 4–5 wt % metallic catalyst particles, and <5 wt % carbon-derivative (amorphous carbon, graphite) impurities. We further purify these nanotubes by dispersing them in water using NaDDBS surfactant ($C_{12}H_{25}C_6H_4SO_3Na$) and magnetically fractionating the suspension to reduce the magnetic catalyst fraction to ~0.3 wt % [14]. The resulting SWNT-NaDDBS suspension is then dialyzed to remove surfactant and ultracentrifuged to pelletize the nanotubes. The pellet is annealed at 1150 °C and then resuspended in water using NaDDBS. Characterization of the resultant nanotube dispersions shows the nanotubes are 90% ± 5% individual SWNTs with average length $L = 516 \pm 286$ nm [15].

For optical measurements, we prepare homogeneous, oriented SWNT gels by mixing and vortexing the SWNT suspensions together with pre-gel ingredients [16], loading them into precision 1.0 cm × 1.0 cm quartz cells, and placing them in the room-temperature bore of a superconducting magnet (Quantum Design PPMS). We then apply a 9 T magnetic field for 45 min to weakly align the nanotubes, and polymerize the pre-gel solution using an ultraviolet lamp to produce homogeneous suspensions [17]. To minimize gel shrinkage, sample cells are sealed

TABLE I. Sample nanotube densities (n) and measured nematic order parameters (S).

	n (mg/ml)	S (± 0.01)
Sample 1	1.43×10^{-3}	0.182
Sample 2	5.68×10^{-2}	0.191
Sample 3	2.93×10^{-2}	0.116
Sample 4	5.85×10^{-2}	0.118

with Teflon and parafilm, and stored at $\sim 5\,°C$ when not in use. Table I lists the samples we study.

We determine the degree of nanotube alignment using polarized Raman scattering for incident light at 532 nm [18]. The G-band family of Raman modes at ~ 1580 cm^{-1} is highly sensitive to nanotube alignment [5,19,20]. Resonant studies on purified, isolated SWNTs in a backscattering geometry, for example, have shown near complete extinction of all the G-band Raman peak intensities for incident and scattered light polarizations orthogonal to the SWNT axis. In our studies, vertically polarized incident light passes through a notch filter and then scatters within the sample gel whose alignment axis is rotated to an angle ϕ with respect to the input polarization direction. Stokes-shifted inelastic backscattering is collected through a laser-blocking bandpass filter, and then is passed through a vertical polarizer (corresponding to the VV geometry). To restrict the gel volume from which light is collected, we use a high numerical aperture lens ($f/\# \sim 1$) to focus and collect light from the sample, and a confocal spatial filter to limit the depth of focus. We account for anisotropic absorption of incident and inelastically scattered light in our analysis of the Raman orientational contrast, and minimize this contribution by collecting Raman data from a small volume within 0.5 mm from the front face of the sample. The excitation power density averages less than 160 W/cm^2 at focus and produces no gel degradation. All data are taken at room temperature and zero magnetic field.

Typical VV Raman spectra are shown in Fig. 1(a). Note that individual G-band peaks are not resolved in our measurement, but have been found to exhibit the same dependence on nanotube orientation [5]. Measurements on a control sample prepared identically but without nanotubes show no measurable G-band Raman response. Figures 1(b) and 1(c) show the G-band peak intensities versus sample rotation for all samples. To infer the degree of nanotube alignment from these data, we consider a single-parameter orientational model [21],

$$f(\theta) = \frac{e^{-A\cos^2\theta}}{\int_{-1}^{1} e^{-A\cos^2\theta} d(\cos\theta)}, \qquad (1)$$

where θ is the polar angle the nanotube axis makes with the alignment field, B. This distribution function describes uniaxial ordering of nanotubes in the alignment
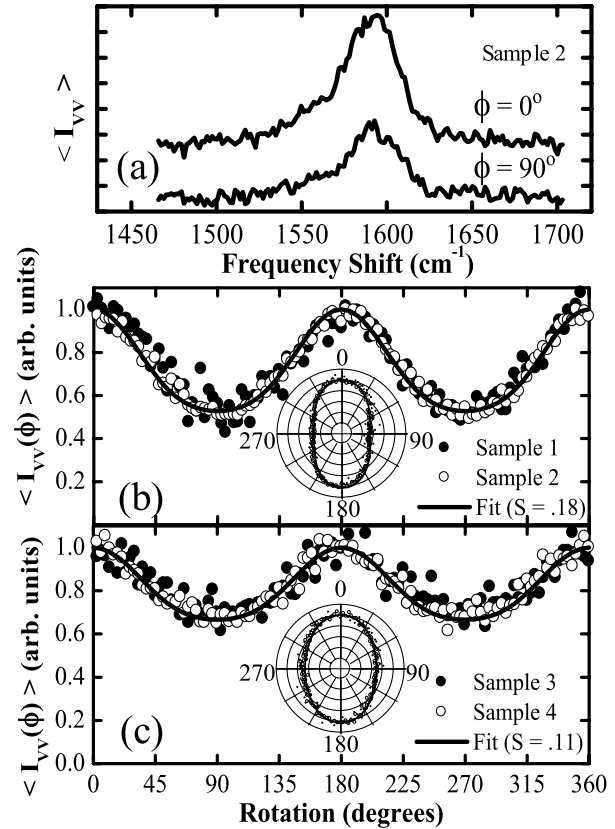

FIG. 1. (a) G-band Raman intensity for sample 2 with VV polarizations parallel and perpendicular to the alignment axis ($\phi = 0$ and 90°, respectively). (b),(c) Raman peak intensity versus sample orientation ϕ for samples 1–4. Insets show polar representations of the same data.

field, and depends on the difference in SWNT magnetic susceptibilities for B parallel and perpendicular to the nanotube axis: $A = (\chi_\parallel - \chi_\perp)B^2/kT$. The VV response of a single nanotube is $I(\alpha) = I_o\cos^4(\alpha)$, where α is the angle between the nanotube axis and the Raman polarization axis [18]. Averaging $I(\alpha)$ over the distribution $f(\theta)$ leads to a predicted Raman intensity $\langle I(\phi)\rangle$, where ϕ is the angle between the alignment field axis and the Raman polarization axis. The parameter A is determined by fitting the measured Raman intensity to this model [Figs. 1(b) and 1(c)]. From this result we compute the nematic order parameter [22],

$$S = \int_{-1}^{1} f(\theta)\left(\frac{3\cos^2(\theta) - 1}{2}\right) d(\cos\theta). \qquad (2)$$

Order parameters resulting from this analysis are shown in Table I. Samples 1 and 2 are prepared together and show a similar degree of alignment. The second batch, samples 3 and 4, exhibits a consistently lower alignment. The latter may arise from a partial initiation of cross linking prior to UV exposure. Taking $S = 0.185 \pm 0.01$ at $B = 9$ T implies a nanotube magnetic

anisotropy of $(6.7 \pm 0.2) \times 10^{-5}$ emu/mol C. Although this number is in reasonable agreement with theoretical predictions of $\sim 1.1 \times 10^{-4}$ emu/mol C for a $(10, 10)$ SWNT [23] and prior experimental measures of SWNT alignment [24], we note that tube alignment may involve other mechanisms such as magnetic torques from permanent moments aligned with the nanotube axis (e.g., from catalyst particles or tube ferromagnetism). Nonetheless, we find that models based on such torques produce similar angular dependence in $f(\theta)$ for $S \ll 1$. Hence, these Raman measurements determine S unambiguously.

These orientations permit us to extract the bare anisotropic optical cross section for these SWNTs despite their incomplete alignment. Figure 2(a) shows the raw optical transmission, $T_\parallel = e^{-n\alpha_\parallel d}$, for light copolarized with the alignment axis. Here, n is the nanotube density, $\alpha_\parallel$ is the absorbance, and $d = 1$ cm is the optical path length. Corresponding data for cross-polarized light, $T_\perp = e^{-n\alpha_\perp d}$, shows a comparably wide range of optical densities. For each polarization, we use a gel without nanotubes in an identical cuvette to obtain reference spectra. Figure 2(b) compares $\alpha_\parallel$ and $\alpha_\perp$ for sample 2. Note that magnetic field alignment of nanotubes results in a marked difference between absorption for the two polarizations, but that spectral features E_{22} and E_{33} associated with the 2-2 and 3-3 SWNT sub-band transitions are apparent in both polarization orientations at ~ 1.4 eV and ~ 1.9 eV, respectively. Moreover, the absorbance polarization $\rho = (\alpha_\parallel - \alpha_\perp)/(\alpha_\parallel + \alpha_\perp)$ [Fig. 3(a)] is different for the first and second batches of samples.

These absorbances are related to the nematic order parameter S and the bare nanotube absorption cross sections $\sigma_\parallel$ and $\sigma_\perp$ according to

$$\alpha_\parallel = \tfrac{2}{3}(\sigma_\parallel - \sigma_\perp)S + \tfrac{1}{3}(\sigma_\parallel + 2\sigma_\perp), \qquad (3)$$

$$\alpha_\perp = -\tfrac{1}{3}(\sigma_\parallel - \sigma_\perp)S + \tfrac{1}{3}(\sigma_\parallel + 2\sigma_\perp). \qquad (4)$$

The quantity $\alpha = \alpha_\parallel + 2\alpha_\perp$ represents the absorbance for an unaligned sample and should be universal for all samples measured despite changes in S and n. Figure 3(b) exhibits this unaligned absorbance derived from measured data, showing reasonable agreement for all samples.

The independently measured sample order parameters now combine with the absorbance data to yield bare nanotube cross sections $\sigma_\parallel$ and $\sigma_\perp$. These data appear in Fig. 4(a) for all samples, and are expected to be universal regardless of changes in nanotube density or degree of alignment among the samples. Given uncertainties in the measured order parameters of $\sim 10\%$, we find good agreement for all measured cross sections. Figure 4(b) shows the data averaged together, representing a calibrated measurement of intrinsic laser-oven nanotube cross sections with an average diameter of 1.35 nm [15]. These data are now sufficiently precise to permit quantitative comparison with theory for the first time.

Optical absorption in SWNTs has been studied theoretically by a number of authors [9,10]. The absorption cross section depends on the imaginary part of the electric polarizability, $P''(\omega)$, through the relation $\sigma(\omega) = 4\pi P''(\omega)\omega/c$. Calculations within a simple linearized noninteracting model of the nanotube electronic structure are shown in Fig. 4(c), for diameters $(1.35 \pm 0.33$ nm) characterized previously [15]. The parallel absorption cross section peaks at energies E_{nn}, while for the perpendicular polarization such diagonal transitions are forbidden and the absorption threshold occurs at E_{12}. Higher
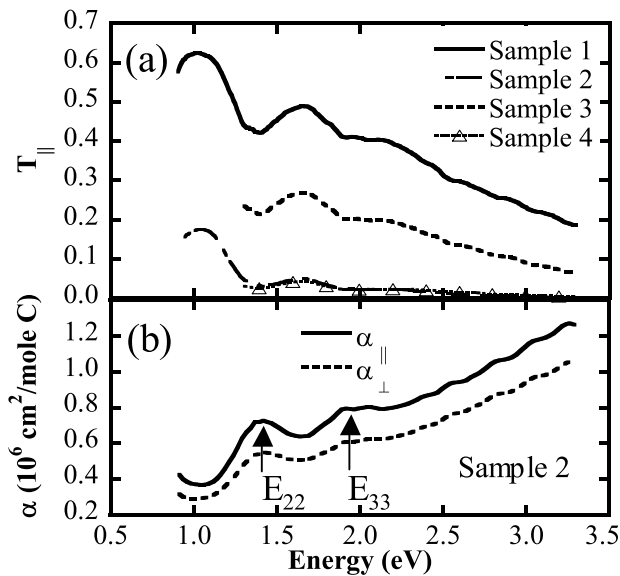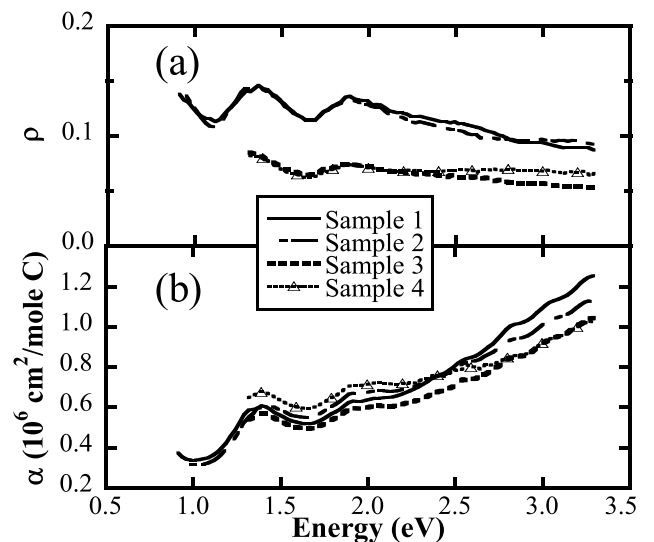

FIG. 2. (a) Raw optical transmission for light copolarized relative to the alignment field axis for all samples. (b) Copolarized and cross-polarized absorbance for sample 2.

FIG. 3. (a) Polarization of absorbance, ρ, and (b) depolarized absorbance, α, for all samples, as defined in the text.
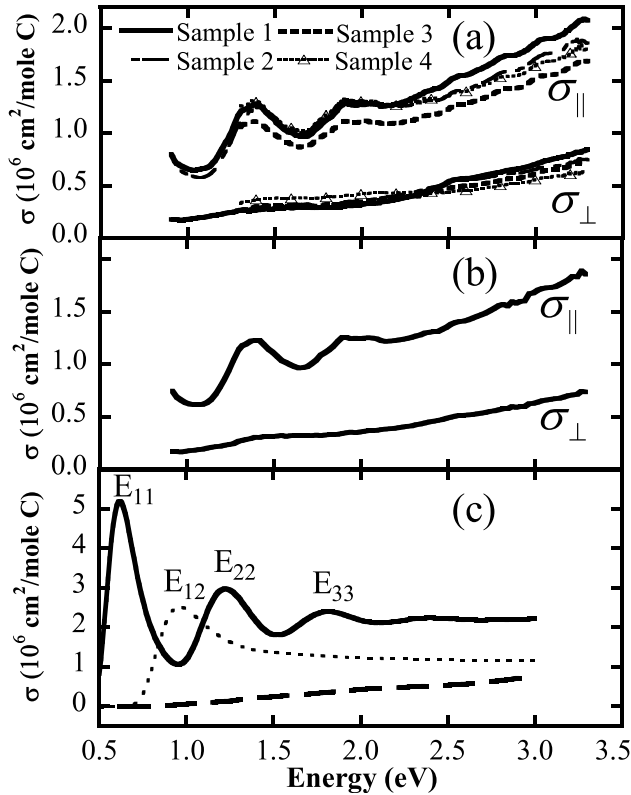
FIG. 4. Bare SWNT optical cross sections for copolarized and cross-polarized light ($\sigma_\parallel$ and $\sigma_\perp$, respectively) for (a) all samples and (b) averaged over all samples. (c) Calculated cross sections for $\sigma_\parallel$ (solid line) and $\sigma_\perp$ with (dashed line) and without (dotted line) a depolarization correction.

peaks in the perpendicular absorption are suppressed due to a vanishing matrix element.

The above calculation ignores electron interactions. While excitons are strongly bound in nanotubes, their binding energy is largely canceled by an increase in the free particle-hole threshold due to interactions [10,25]. Consequently, the net absorption energy is moderately enhanced over the noninteracting prediction. For the purpose of our ensemble averaged calculation this effect can be accounted for by phenomenologically adjusting the graphene Fermi velocity.

For a perpendicular electric field, the induced charges on the surface of the nanotube produce a depolarizing field inside the nanotube that largely cancels the external field [9]. This leads to a screened polarizability, $\tilde{P}(\omega) = [P^{-1}(\omega) + 2/LR^2]^{-1}$, where L is the nanotube length and R its radius. This effect substantially reduces the perpendicular absorption and eliminates the peak associated with E_{12} [Fig. 4(c)]. Such local field suppression does not occur in the parallel field because the induced charges occur only at the ends of the nanotube [10]. Our observations thus explicitly demonstrate the depolarization effect due to screening by induced charge.

In conclusion, we combine Raman and absorption spectroscopy to determine energy-dependent SWNT ab-

solute linear absorption cross sections and anisotropies. These data provide a benchmark for quantitative tests of theory, and show clear evidence for the absence of sub-band features in the cross-polarized channel, as predicted by local field depolarization effects. The cross sections will permit simple absorbance measurements to assign alignment order parameters to nanotube suspensions immersed in external fields (e.g., magnetic, electric, shear) and to nanotube composites.

[1] T.W. Odom et al., Nature (London) **391**, 62 (1998); P. L. McEuen, Phys. World **6**, 31 (2000).
[2] J. Hone et al., Phys. Rev. B **59**, R2514 (1999).
[3] M. M. Treacy et al., Nature (London) **381**, 678 (1996); J.-P. Salvetat et al., Phys. Rev. Lett. **82**, 944 (1999).
[4] A. Jorio et al., Phys. Rev. Lett. **85**, 2617 (2000).
[5] G. S. Duesberg et al., Phys. Rev. Lett. **85**, 5436 (2000).
[6] J. Hwang et al., Phys. Rev. B **62**, R13 310 (2000); Z. M. Li et al., Phys. Rev. Lett. **87**, 127401 (2001).
[7] M. J. O'Connell et al., Science **297**, 593 (2002); S. M. Bachilo et al., Science **298**, 2361 (2002).
[8] R. Saito, G. Dresselhaus, and M. S. Dresselhaus, *Physical Properties of Carbon Nanotubes* (Imperial College Press, London, 1999).
[9] H. Ajiki and T. Ando, Physica B (Amsterdam) **201**, 349 (1994).
[10] T. Ando, J. Phys. Soc. Jpn. **66**, 1066 (1997).
[11] S. Fan et al., Science **283**, 512 (1999); J. Kong et al., Science **287**, 622 (2000); B. Vigolo et al., Science **290**, 1331 (2000).
[12] Tubes@Rice laser-oven SWNTs, batch P081600.
[13] A. G. Rinzler et al., Appl. Phys. A **67**, 29 (1998).
[14] M. F. Islam, D. E. Milkie, O. N. Torrens, A. G. Yodh, and J. M. Kikkawa (to be published).
[15] M. F. Islam et al., Nano Lett. **3**, 269 (2003).
[16] M. F. Islam et al., Phys. Rev. Lett. **92**, 088303 (2004).
[17] A radiant power density of ~1 mW/cm² at 385 nm for 3 min is sufficient to prevent tube reorientation.
[18] H. H. Gommans et al., J. Appl. Phys. **88**, 2509 (2000).
[19] A. Hartschuh et al., Phys. Rev. Lett. **90**, 095503 (2003).
[20] A. Jorio et al., Phys. Rev. B **65**, 121402 (2002).
[21] M. Fujiwara et al., J. Phys. Chem. A **105**, 4383 (2001).
[22] P. M. Chaikin and T. C. Lubensky, *Principles of Condensed Matter Physics* (Cambridge University Press, Cambridge, 1997), 2nd ed.
[23] J. P. Lu, Phys. Rev. Lett. **74**, 1123 (1995).
[24] D. A. Walters et al., Chem. Phys. Lett. **338**, 14 (2001).
[25] C. L. Kane and E. J. Mele, cond-mat/0403153.